Journal of Sound and Vibration ▮ (▮▮▮▮) ▮▮▮–▮▮▮

Contents lists available at ScienceDirect

Journal of Sound and Vibration

journal homepage: www.elsevier.com/locate/jsvi

Transient friction-induced vibrations in a 2-DOF model of brakes

Valery Pilipchuk [a], Paweł Olejnik [b,*], Jan Awrejcewicz [b]

[a] Department of Mechanical Engineering, Wayne State University, 5050 Anthony Wayne Drive, Detroit, MI 48202, USA
[b] Department of Automation, Biomechanics and Mechatronics, Lodz University of Technology, 1/15 Stefanowski Street, 90-924 Lodz, Poland

ARTICLE INFO

Article history:
Received 15 May 2014
Received in revised form
14 January 2015
Accepted 21 January 2015
Handling Editor: L.N. Virgin

ABSTRACT

Non-stationary effects in the friction-induced dynamics of a two-degree-of-freedom brake model are examined in this paper. The belt–spring–block model is designed to take into account variations of the normal load during the braking process. It is shown that due to the adiabatically slowing down velocity of the belt, the system response experiences specific qualitative transitions that can be viewed as simple mechanical indicators for the onset of squeal phenomenon. In particular, the creep-slip leading to a significant widening of the spectrum of the dynamics is observed at the final phase of the process.

1. Introduction

This paper deals with friction-induced vibrations that may occur, for instance, in different brake systems during deceleration. Such types of problems are of significant interest in the literature due to clear practical reasons, complexity of physical effects, and mathematical challenges of the modeling; see publications [4,8,16,17] for an overview of the problem's status. The idea of considering the decelerating sliding is due to the fact that the brake squeal phenomenon is usually observed at the final stage of braking process. Practically, the deceleration is very slow as compared to the temporal scales of friction induced vibrations associated with elastic modes of braking systems. This enables one of ignoring the corresponding inertia forces when considering different transitional effects caused by the decay of relative speed at the friction interface. Modeling such transitional effects is important for understanding physical conditions of the onset of squeal phenomenon including possible mechanisms of excitation of acoustical modes. Although describing the acoustical squeal effects in terms of reduced few degrees-of-freedom mechanical models seems unrealistic by many reasons, it is important to find simple analogues of squeal conditions by keeping the key physical features of real brake systems. In particular, based on the standard block–spring model on a moving belt, it was found earlier that stick-slip (or creep/slip) vibrations, captured at some low enough belt speed, are preserved during further deceleration by showing increasing temporal localization of slip phases [25]. This leads to widening spectrum of the dynamics, which can provide the possibility of interaction with acoustical modes in real brake systems.

Such effects obtained experimental proof based on the rig designed in [9,21], however, theoretical considerations of the present work are conducted on a new model, which accounts for the influence of gravity and geometrical nonlinearity.

Friction-induced vibrations in physical systems based on the mass—damper–spring modeling have been widely considered in the literature for many years. In particular, such models have been used extensively as deterministic

* Corresponding author.
E-mail address: pawel.olejnik@p.lodz.pl (P. Olejnik).

http://dx.doi.org/10.1016/j.jsv.2015.01.028
0022-460X/

simulators of earthquakes [27]. The earthquake generation mechanism as a chaotic phenomenon in a two-degree-of-freedom autonomous system with static and dynamic friction was illustrated in [15] by using the Poincaré map diagrams showing, in many cases, a complicated chaotic behavior of the model. It was found that even perfectly symmetric systems possess complicated quasi-periodic orbits with significant out-of-phase components. Due to the specific temporal behavior of stick-slip phenomena [12,26] such components may lead to asymmetric broadband loads and therefore excite flexural vibration modes/waves in both interacting parts.

A two-degree-of-freedom oscillator combining rotational and translational friction-induced vibrations and taking into account geometrical nonlinearity was investigated in [6,7] by means of classical numerical tools based on Newton's and shooting methods. In particular, Floquet multipliers, which are responsible for stability and bifurcations of periodic orbits, were obtained. In particular, it was shown that both regular and chaotic dynamics including different sticking and slipping phases are possible.

Based on a numerical study of four degrees-of-freedom model, it was found in [18] that the motion of the system transverse to the direction of braking experiences a sharp change in excitation leading to a complicated vibration when the slip velocity in the braking direction is low. The authors interpret the disc brake squeal as a friction induced phenomenon caused by the transient, dissipative nature of a braking process.

Different spring–block friction models were used in order to examine the role of friction in the instability mechanism [10,19,20,23]. Based on a model of continuous and discrete elastic elements, the self-excited oscillation in two surfaces sliding against each other was investigated in [1]. Radiation of plane body waves caused by friction was considered in [2]. Some of the results support the interpretation that certain friction behavior is a consequence of the dynamics of the interacting systems rather than the interfacial properties. Contact modeling with emphasis on the contact forces and their relationships to the geometrical, material and mechanical properties of the contacting bodies was reviewed in [3]. Applied aspects of friction-induced vibration and related stability problems are discussed in reviews [16,17,29,31].

This paper deals with the transient dynamics of a two-degree-of-freedom system due to the deceleration of the belt carrying just one of the two inertial elements of the model. Note that the case of decelerating sliding is practically important because deceleration is often caused by friction. For instance, stick-slip instabilities in a decelerating two-degree-of-freedom mass–spring system with one mass subjected to friction were considered earlier in [32]. The research was motivated by the necessity to avoid stick-slip effects in engineering practice. Effects of four different discontinuous friction laws on the system response were investigated. Based on numerical solutions, it was concluded that the existence of stick-slip in decelerated motions depends mainly on the properties of the mechanical systems rather than on the characteristics of the frictional force. In particular, it was noted that rapid and abrupt changes from stick to slip motions and vice verse induce a broadband excitation spectrum leading to squeal, rattling and possibly damage. A mechanical system with two elastically connected masses moving vertically in a cylindrical tube under gravity and subjected to friction with the tube was considered in [33]. In this case of accelerated sliding, it was found that after some transient period, the dynamics is stabilized with regular oscillation of the relative mass displacements.

It should be noted that rigid body models involving few degrees of freedom are generally not sufficient to adequately describe friction-induced phenomena at friction interface. However, numerous experimental results have clearly shown that dominant spikes of the 'squealing spectrum' occur at a few frequencies or sometimes just one frequency. Therefore only a few vibration modes may eventually be involved in the interaction dynamics.

A two-degree-of-freedom mass–damper–spring model interacting with a decelerating rigid strip is analyzed in the present work. As mentioned at the beginning of the present section, such mechanical model was designed in [21] to account for variations of the normal pressure at friction interface within elastic degree-of-freedom in the easiest way. This model can be viewed as a modified version of four degrees-of-freedom plane mechanical system introduced in [5] to take into account both force decreasing segment of the friction law and the change of the normal force generated by the rigid body movement. The proposed model combines a main block connected to base and an angular swinging body by linearly elastic springs; see Fig. 1a. The main block is directly excited by the friction force due to the moving belt, while the role of the angular body is two-fold. Namely, it represents an extra degree-of-freedom in the horizontal plane of main block while creating a variable component of the normal load on the main block due to another (vertical) spring attached to the main block and another end of the angular body. For theoretical study, however, we generalize the mathematical model suggested [21,8] in order to account for geometrical nonlinearities and the influence of gravity. Our study focuses on investigating non-stationary (transient) effects and the corresponding evolution of the spectral characteristics of the dynamics caused by deceleration of the moving belt. Experimental validation is based on comparison of experimental and theoretical time history records for the dynamic states and the corresponding Fourier spectrograms. The spectrograms appeared to be a convenient for illustration of slow changes in spectral properties of the high-frequency friction-induced vibrations.

2. The model description and preliminary analyses

2.1. Design of experimental rig and test setup

A general view on the experimental rig and schematic diagram for mathematical modeling are given in Fig. 1. The designed laboratory rig approximates the real braking system through the feedback reinforcement of the friction force acting on the vibrated block. The feedback reinforcement of the friction force is provided by the increase of vertical load on

Please cite this article as: V. Pilipchuk, et al., Transient friction-induced vibrations in a 2-DOF model of brakes, *Journal of Sound and Vibration* (2015), http://dx.doi.org/10.1016/j.jsv.2015.01.028

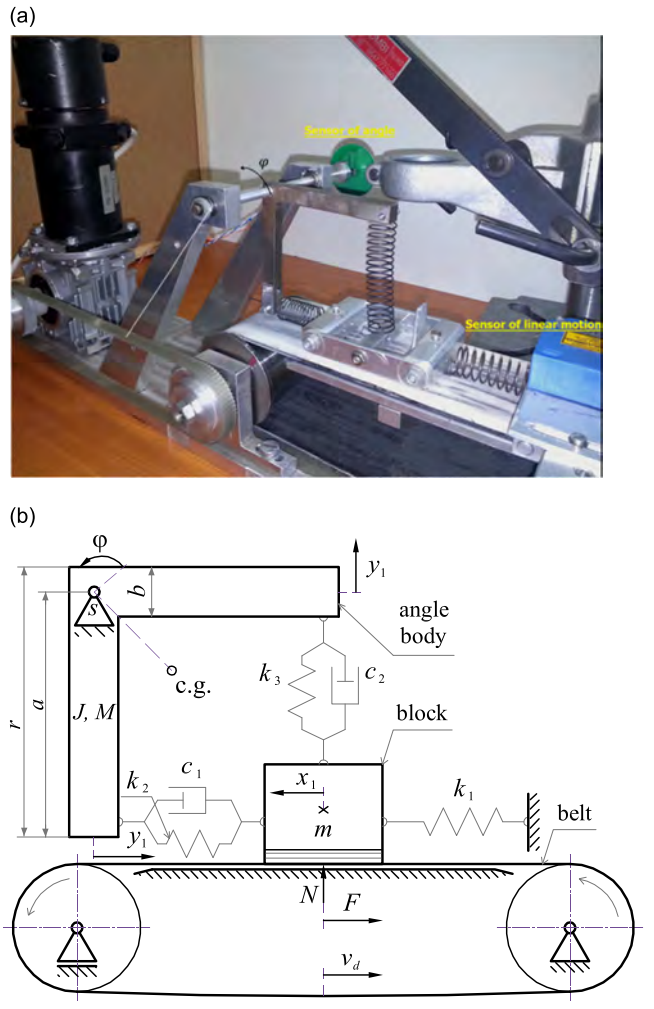

Fig. 1. Mechanical model of a braking system [21]: (a) experimental rig and (b) theoretical model.

the block through the angle body with the set of connecting springs and dampers. When the belt moves the block to the right, the angle body rotates counterclockwise causing compression of the vertical spring and inducing the vertical damping force. Such mechanism associates with the functionality drum brake in a real brake system [8].

Earlier, a laboratory rig was designed for observations and experimental research of frictional effects including the friction force measurement [21]. With reference to Fig. 1a, the block of mass m is moving on the belt in the direction x_1, and the angle body, whose mass and moment of inertia are M and J, respectively, is rotating around point S. The two bodies of the system are coupled by linear springs k_2 and k_3; the block on the belt is additionally coupled to the ground base by means of the linear spring k_1. There is no external loading applied to the angle body, except the gravity. The rotational motion of the angle body is damped by virtual dashpots c_1 and c_2 characterizing air and bearing resistance. It is assumed that the angle of rotation of the angle body is small enough, and varies within the range $|\varphi| < 5^\circ$. In this case, the rotation is approximated by the linear displacement y_1 of the ends of angle body as shown in Fig. 1b. The belt is moving with the velocity $v_b(t)$ assuming no deformation of the belt in the stick-slip contact zone. A non-stretchable 25 mm thick belt made of hard rubber is placed on solid shafts and supported by a flat bar under the examined (main) block. The propeller shaft is installed in a floating manner to avoid belt's tension, and the rig is essentially equipped with a direct current commutator motor PZTK 60-46 J, which is suitable for using in cross-feed drives of numerically controlled machines, supplied by voltage 30 V and possible current load up to 4.1 A.

In addition, stabilization and control of the motor rotational velocity is by the RN12 regulator, which also serves as an amplifier.

The system coordinates, such as displacement of the block and rotation of the equal-bar angle body, are detected by the non-sticking measurement method, in which the laser proximity switch is assigned to measure the displacement of the main block. A Hall-effect device, whose principle of operation is based on variations of the magnetic field, is used to detect the rotation of angle body. It should be emphasized that both sensors have linear characteristics of the measured quantity

Please cite this article as: V. Pilipchuk, et al., Transient friction-induced vibrations in a 2-DOF model of brakes, *Journal of Sound and Vibration* (2015), http://dx.doi.org/10.1016/j.jsv.2015.01.028

versus voltage output. Also, all the sub-components of the laboratory rig are attached to a stable frame. Analog signals acquired from the sensors are processed through a PCI card interfaced by chassis SCXI-1000 with terminals NI-1321 and NI-1302 with the LabView software by dynamic acquisition using test instruments made by National Instruments.

The stored data are indicated on panel-situated scalable charts. Disturbances of the whole structure, noise in electrical circuits, and other additional effects have significant influence on the accuracy of measured signals. Therefore, signals are digitally filtered by a point-by-point polynomial interpolation. It makes significant smoothing of the time histories, but sensitivity of the filtering is controlled by the amount of points from raw data acquisition taken in the interpolation procedure.

Further data analysis is conducted in Matlab interface as described below in Section 4.

2.2. Mathematical modeling

The differential equations of motion of the two-degree-of-freedom mechanical system under consideration are derived by incorporating generalized non-conservative forces into Euler–Lagrange equations of the corresponding conservative system. A schematic diagram of the model is shown in Fig. 1b. The main (horizontal) block is driven longitudinally by the moving belt by friction forces. The load transfer between the main block of mass m and the angular body is provided by the spring k_2 and damper c_1 while the normal load from the rotating angular body on the main block is transferred by the vertical spring k_3 and damper c_2. The moment of inertia of the angular body with respect to its center of rotation S is J and the total mass is M. The main block is also connected to the base by the spring of stiffness k_1.

Absolute deformation of the spring k_1, which remains horizontal during its tension-compression, is simply equal to the displacement of block m. Elongations of the two other springs, k_2 and k_3, are calculated as $\Delta l_2 = \sqrt{(l_0-x_1-y_1)^2+r^2(1-\cos\varphi)^2}-l_0$ and $\Delta l_3 = \sqrt{x_1^2+(r+y_1)^2}-r$, respectively, where l_0 is the original length of spring k_2, and the original length of spring k_3 is assumed to be equal to r as justified in Fig. 1a. Assuming that the coordinates x_1 and y_1 are of the same order of magnitude, the angle φ is small enough, taking into account that $r^2(1-\cos\varphi)^2 \sim y_1^4/r^2$, and ignoring the third and higher degree terms in the power series expansions with respect to the coordinates brings spring deformations to the form

$$\Delta l_1 = x_1, \tag{1a}$$

$$\Delta l_2 = -z_1, \tag{1b}$$

$$\Delta l_3 = y_1 + \frac{x_1^2}{2r}, \tag{1c}$$

where $z_1 = x_1 + y_1$, and high powers of the displacements in the expressions for Δl_2 and Δl_3 are ignored.

Assuming that all the springs are linearly elastic, the Lagrange function of the corresponding conservative system is represented in the form

$$L = \frac{1}{2}\left(m\dot{x}_1^2 + J\dot{\varphi}^2\right) - \frac{1}{2}\left(k_1\Delta l_1^2 + k_2\Delta l_2^2 + k_3\Delta l_3^2\right) - P(\varphi), \tag{2}$$

where $P(\varphi) = Mgl\left[1-\cos(\pi/4+\varphi)\right]$ is the potential energy of angular body accumulated due to the elevation of its center of gravity (c.g.) with respect to its equilibrium position at the absence of springs, $\varphi = -\pi/4$. The angular displacement can be approximated by $\varphi = y_1/r$, and the distance between the center of rotation and c.g. is estimated as $l = (3\sqrt{2}/4)r$.

The virtual work done against dissipation/resistance forces is

$$\delta A = F\delta x_1 + Q\delta\varphi + c_1\dot{z}_1\delta z_1 + c_2\dot{y}_1\delta y_1, \tag{3}$$

where $\dot{z}_1 = \dot{x}_1 + \dot{y}_1$, F is the friction force between the main block and the moving belt, and Q is the resistance torque at the suspension point S, which can be caused by dry friction, viscous damping, and some elastic forces; and $\delta\varphi = \delta y_1/r$ as soon as the rotation angle is small enough according to the assumption.

Generalized Euler–Lagrange equations of motion are derived in the following form:

$$\frac{\mathrm{d}}{\mathrm{d}t}\frac{\partial L}{\partial \dot{x}_1} - \frac{\partial L}{\partial x_1} = -\frac{\delta A}{\delta x_1}, \tag{4a}$$

$$\frac{\mathrm{d}}{\mathrm{d}t}\frac{\partial L}{\partial \dot{y}_1} - \frac{\partial L}{\partial y_1} = -\frac{\delta A}{\delta y_1}, \tag{4b}$$

where the right-hand side represents generalized forces associated with the virtual work described by Eq. (3). Substituting (2) and (3) in (4) gives

$$m\ddot{x}_1 + c_1\dot{z}_1 + (k_1+k_2)x_1 + k_2y_1 + k_3\frac{x_1}{r}\left(y_1 + \frac{x_1^2}{2r}\right) = -F, \tag{5a}$$

Please cite this article as: V. Pilipchuk, et al., Transient friction-induced vibrations in a 2-DOF model of brakes, *Journal of Sound and Vibration* (2015), http://dx.doi.org/10.1016/j.jsv.2015.01.028

$$\frac{J}{r^2}\ddot{y}_1+c_1\dot{z}_1+c_2\dot{y}_1+k_2z_1+k_3\left(y_1+\frac{x_1^2}{2r}\right)+Mg\lambda_r=-\frac{Q}{r}, \tag{5b}$$

where

$$\lambda_r=\frac{\sqrt{2}}{2}\frac{l}{r}\left(1+\frac{y_1}{r}-\frac{y_1^2}{2r^2}-\frac{y_1^3}{6r^3}\right)$$

and the friction force F depends upon variations of the vertical load as follows:

$$F=\mu mg\left(1+\frac{M}{m}\lambda_r-\frac{k_3}{mg}\left(y_1+\frac{x_1^2}{2r}\right)-\frac{c_2}{mg}\dot{y}_1\right). \tag{6}$$

The friction law, which is the dependence of friction coefficient on the relative velocity at the friction interface, $V_{\rm rel}=\dot{x}_1-v_b$, is given by

$$\mu(V_{\rm rel})=\frac{\mu_0}{1+\gamma|V_{\rm rel}|}\left(1+\frac{\beta}{\cosh\alpha V_{\rm rel}}\right)\tanh\alpha V_{\rm rel}, \tag{7}$$

where μ_0 is a constant parameter controlling the 'amplitude' of spike in the friction coefficient, assuming that the range of relative velocities is narrow enough, the parameter γ is responsible for the decay of friction force as the modulus of relative velocity is increasing, α controls the curve's sharpness near zero, and finally β controls the magnitude of spikes near zero, in other words, the rate of original drop of the friction coefficient just after the main mass quits the 'creeping' area. In particular, the thin line in Fig. 2 illustrates the shape of friction law at $\mu_0=0.5$, $\gamma=3.0$, $\alpha=200.0$, and $\beta=0.7$. Such parameters are chosen below for numerical simulations.

If $\gamma=0$, the friction law (7) becomes similar to that introduced in [25] for modeling the so-called "creep-slip" dynamics of a typical 2-DOF mass–spring model on a moving belt within the class of smooth functions. In this case, the curve peaks can be found analytically as follows.

Differentiating (7) with respect to $V_{\rm rel}$ gives

$$\mu'(V_{\rm rel})=\alpha\mu_0\,\mathrm{sech}(V_{\rm rel}\alpha)\left[2\beta\,\mathrm{sech}^2(V_{\rm rel}\alpha)+\,\mathrm{sech}(V_{\rm rel}\alpha)-\beta\right]=0.$$

Therefore, peak locations are determined from the following quadratic equation with respect to $\mathrm{sech}(V_{\rm rel}\alpha)$:

$$2\beta\,\mathrm{sech}^2(V_{\rm rel}\alpha)+\mathrm{sech}(V_{\rm rel}\alpha)-\beta=0.$$

This eventually gives four roots for $V_{\rm rel}$ of which only two are real

$$V_{\rm rel}=\pm V^*,\quad V^*=\frac{1}{\alpha}\mathrm{arcsech}\left(\frac{\beta_0-1}{4\beta}\right),\quad \beta_0=\sqrt{1+8\beta^2}. \tag{8}$$

Now, substituting Eq. (8) in (7) gives the peak magnitudes

$$\mu^*=\pm\frac{\mu_0}{16\beta}\sqrt{\frac{\beta_0-3\beta}{1-\beta}}(3+\beta_0)(\beta_0-1+4\beta). \tag{9}$$

The factor $1/(1+\gamma|V_{\rm rel}|)$ in (7) is added in order to better capture the decaying intervals outside the narrow area between positive and negative spikes of the curve. Such decays were observed in the previous tests conducted with the same experimental rig [8,9]. Note that there are very many friction laws suggested in the literature possibly due to the fact that behavior of friction force depends upon individual geometrical and physical properties of real interacting bodies as well as environmental conditions. Usually typical curves are used for pure theoretical studies, however, the present work deals with comparison of the modeling and experimental results. In such case, the friction law must be as close as possible to that

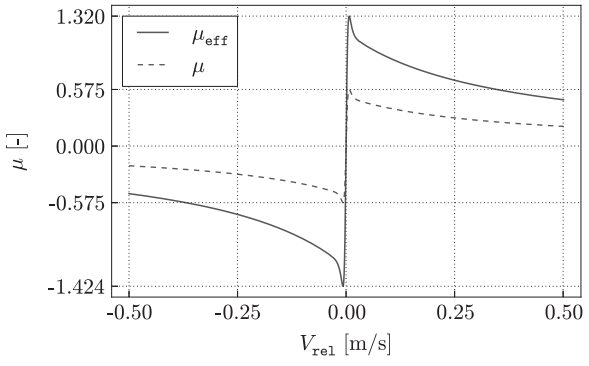

Fig. 2. Friction coefficient and friction interface (dashed line), and the effective friction coefficient of the model (solid line) obtained under the following parameter values: $\mu_0=0.5$, $\gamma=3.0$, $\alpha=200.0$, $\beta=0.7$.

Please cite this article as: V. Pilipchuk, et al., Transient friction-induced vibrations in a 2-DOF model of brakes, *Journal of Sound and Vibration* (2015), http://dx.doi.org/10.1016/j.jsv.2015.01.028

observed on the system under consideration.

Quick variations of the friction coefficient in the neighborhood of zero relative speed constitutes the most common physical phenomenon, which is responsible for important qualitative features of the dry friction dynamics, in particular, stick-slip vibration. The idea of modeling the dry friction coefficient by simple discontinuous functions enables one to approximate the strongly nonlinear characteristics by combining exact analytical expressions for physically different regimes of the friction process [28]. However, this non-analytic relation of the friction force versus the relative speed requires different differential equations to be used for describing the dynamics in different regions of the phase space. The corresponding formulations appear to be mathematically challenging [14] and require suitable conditioning for the numerical integration since a single form of the differential equation of motion cannot be derived in this case.

Alternatively, exponential functions can be employed to approximate the abrupt changes of the friction coefficient [10,11,13,16,17,24,30]. An obvious advantage of these analytic expressions is the direct application of nonlinear vibration techniques such as expansion and perturbation methods. From a physical viewpoint, the static friction is considered as a viscous force with a very large coefficient of viscosity.

Note that the strongly viscous region $|V_{\rm rel}| \le V^*$ represents a relatively narrow domain of creeping (quasi-sticking) motion. According to Ref. [27] (see also references therein), such an area is presumably a necessary component of any realistic friction law. The creeping area was represented by a linear viscosity assumption such that the friction law had a 'kink' in transiting from the 'sticking' regime to the 'slipping' regime, and remained as a non-smooth function of the relative speed.

The adapted law has no 'static point' but a very narrow creeping interval. This may not be a good curve for modeling friction interactions of stiff surfaces, such as metals and ceramic. However, it seems to be well justified when at least one of the surfaces is relatively soft. In our experimental rig, the belt is made of a rubber type polymer material whose properties are represented by the friction law rather than the belt itself for simplicity reason. Discontinuous friction curves are correct from an engineering standpoint and can be indeed handled by the conditioning (event detection) during numerical integration. However, the presence of discontinuities in the differential equations of motion may be questioned from the standpoint of existence and uniqueness of solution including the so-called the Lipschitz condition. A numerical procedure with detection of events in the dynamics of similar 2-DOF mechanical system with dry friction was used by the authors in [22].

Let us assume the steady-state conditions at constant belt's speed and obtain an effective friction coefficient, which takes into account the influence of the angular body as shown in Fig. 1. Ignoring the inertia and viscosity forces and solving linearized equations (5) and (6) with respect to F, x_1 and y_1 gives the effective friction coefficient

$$\mu_{\rm eff} = \frac{F}{mg} = \frac{(1+\kappa_1)\mu}{1+\kappa_2\mu}, \tag{10}$$

where

$$\kappa_1 = \frac{3Mr\left[k_1k_2+2(k_1+k_2)k_3\right]}{m\kappa_3}, \quad \kappa_2 = \frac{4rk_2k_3-3Mgk_2}{\kappa_3},$$
$$\kappa_3 = 3Mg(k_1+k_2)+4r\left[k_2k_3+k_1(k_2+k_3)\right].$$

The curve of effective friction coefficient (10) is shifted downward as illustrated in Fig. 2 and has as many as twice larger amplitudes, which is caused by both structural and physical specifics of the model. It is shown in the next section that the asymmetry of the effective friction coefficient affects the system dynamics.

3. Conditions of experimental and numerical tests

In order to numerically illustrate the effect under consideration, let us chose the experimentally estimated model parameters [21] as follows: $M = 0.14027$ kg, $m = 0.1052$ kg, $J = 2.4423 \times 10^{-4}$ kg m^2, $r = 0.078$ m, $k_1 = 367.0$ N m^{-1}, $k_2 = 76.0$ N m^{-1}, $k_3 = 69.0$ N m^{-1}, $c_1 = 0.0156$ N s m^{-1}, $c_2 = 0$. In this case, the corresponding linearized conservative system has the following eigen-frequencies: $\omega_1 = 9.87007$ Hz and $\omega_2 = 14.1971$ Hz. Therefore, in contrast to the reference [25], no low-order internal resonances are assumed here. In order to provide 'adiabatic' loading conditions, let us consider the case of slowly decelerating belt whose speed is decaying by the linear law

$$v_b(t) = V_0\left(1-\frac{t}{T_{\max}}\right), \tag{11}$$

where $V_0 = 0.17$ m s^{-1} is the initial speed and $T_{\max} = 45$ s is the duration of process; based on such parameters, the speed (11) can be considered as slowly varying in the temporal scale of eigen-vibrations of the model.

Eqs. (5) therefore can be rewritten in the general standard form

$$\dot{x}_1 = x_2, \tag{12a}$$

$$\dot{x}_2 = f(x_1, x_2, y_1, y_2, t), \tag{12b}$$

$$\dot{y}_1 = y_2, \tag{12c}$$

Please cite this article as: V. Pilipchuk, et al., Transient friction-induced vibrations in a 2-DOF model of brakes, *Journal of Sound and Vibration* (2015), http://dx.doi.org/10.1016/j.jsv.2015.01.028

$$\dot{y}_2 = g(x_1, x_2, y_1, y_2), \tag{12d}$$

where the function f depends explicitly on the time parameter t in a slow (adiabatic) way through the belt speed (11).

The above listed values of parameters are close to those obtained by measurements for the experimental rig, which is shown in Fig. 1a. Note that some of the important parameters are hardly possible to identify exactly due to both geometrical and physical issues. For instance, it is known that friction-induced dynamics is quite sensitive to parameters of friction laws and shapes of the corresponding curves. Also, the real block interacting with the moving belt is a three-dimensional body creating a non-homogeneous distribution of the normal pressure on the belt across the bottom surface of the block. In addition, the belt speed is difficult to control exactly to match the target (11). The main purpose of the present study is to find qualitative agreement between the theoretical and experimental results describing the major transitional effects in decelerating sliding, rather than to achieve a perfect quantitative match between the dynamic states.

4. Evolution of the creep-slip response

Preliminary illustration and some comparison of the theoretical and experimental results are given in Fig. 3.

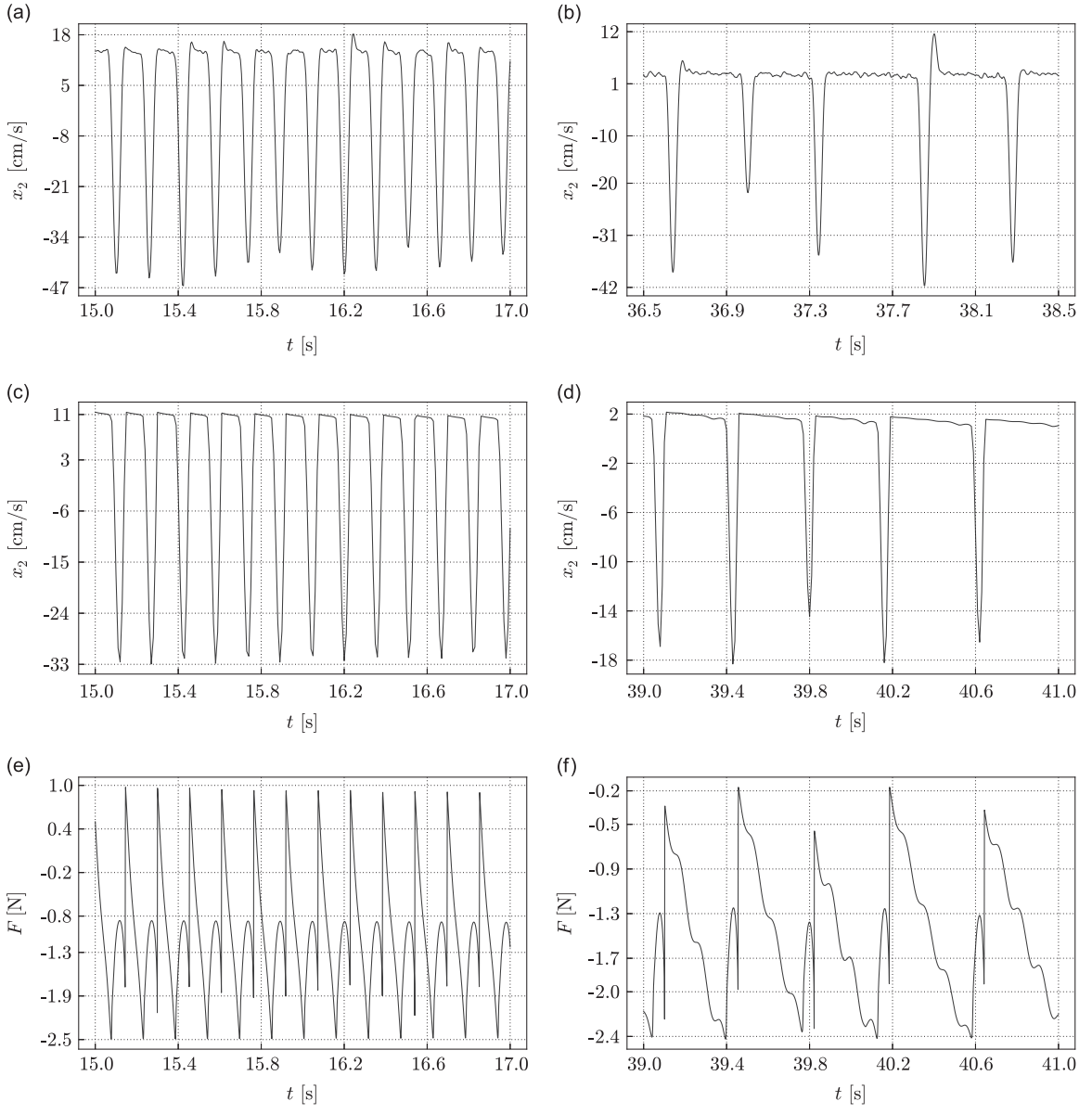

Fig. 3. Different short-term time histories in windows of two seconds: (a and b) velocity of the main block obtained from experiment, (c and d) velocity of the main block obtained from the modeling, and (e and f) friction force obtained from the modeling.

Please cite this article as: V. Pilipchuk, et al., Transient friction-induced vibrations in a 2-DOF model of brakes, *Journal of Sound and Vibration* (2015), http://dx.doi.org/10.1016/j.jsv.2015.01.028

Fig. 3a–d illustrates the velocity of main block $x_2 = \dot{x}_1$ obtained from the test and numerical solution of (12). The time histories are shown in time windows of 2 s covering the developed and final phases of the dynamics. Both the experiment and the simulation show the typical spike-wise behaviors of the velocity, which is usually observed during creep-slip vibrations. Due to the deceleration of the moving belt, the intervals between spikes are increased by the end of the process as it is seen from comparison of Fig. 3a, c and e. Increasing irregularity of the spike amplitudes is also seen near the end of the process. These are the factors leading to the widening of spectrum of the dynamic states as will be illustrated in detail below in Section 5. Note that the friction force, which is obtained from the modeling, is shifted downward into the negative area; see Fig. 3e and f. When the spikes become widely spaced, the friction force develops a small high-frequency component in creeping phases as seen from the fragments d and f of Fig. 3. Such component is caused by the variation of vertical load on the main block due to the rotational vibrations of the angular body. These vibrations are excited by sudden slips of the main block through the horizontal and somewhat vertical springs as follows from the form of (5).

In order to directly characterize transient effects in spectral properties of the dynamics, the Fourier spectrogram tool is applied to the coordinate and velocity of the main block. This sub-component is directly excited by the friction force and therefore represents the major source of dynamic excitation to the rest of the system. The Matlab procedure

```
[S, F, T, P] = spectrogram(signal, 512, 256, [ ], 1E2)
surf(T, [ ], 10*log10(P), 'edgecolor', 'none')
```

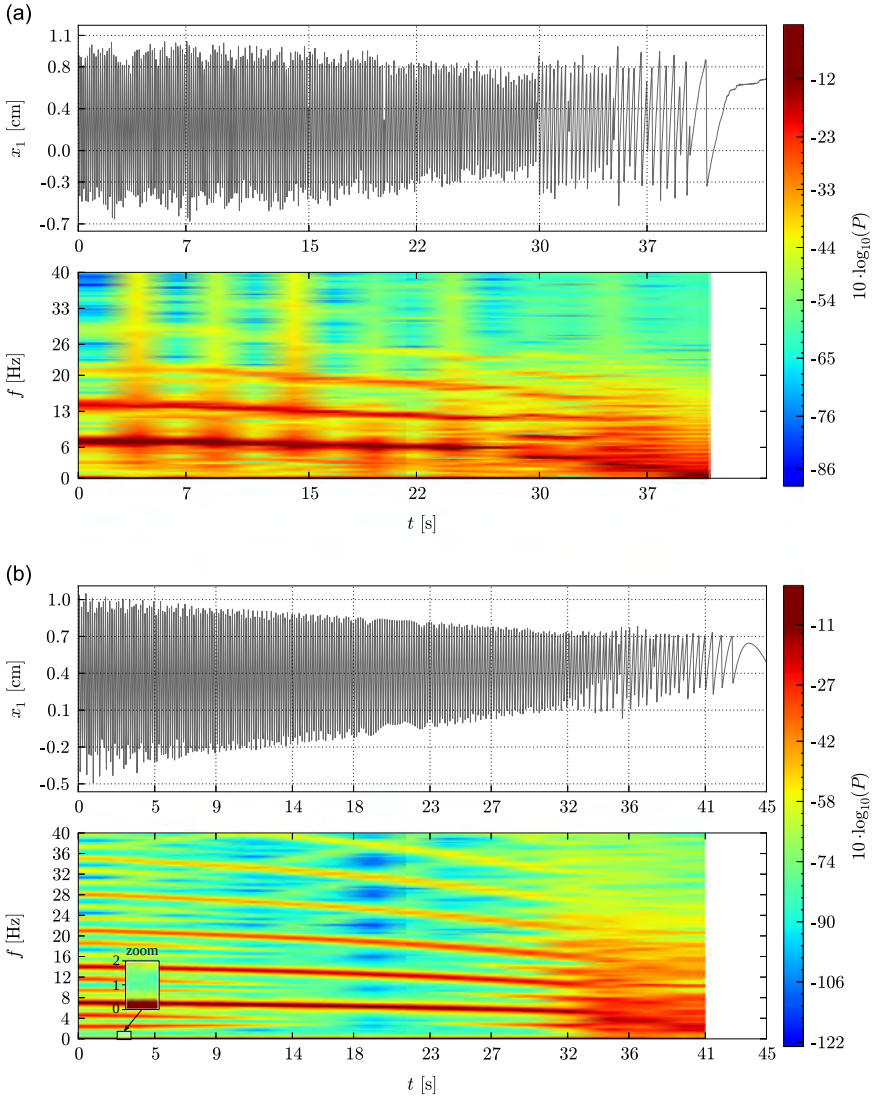

Fig. 4. Time histories of the main body coordinate with the corresponding Matlab spectrograms obtained from (a) test and (b) numerical simulation for the theoretical model; three major spectral lines at the bottom correspond to the constant shift of the main block from its initial position, and two principal frequencies, which are close to those of the linearized conservative system; colors illustrate the power spectral density in logarithmic scale, $10\log_{10}P$. (For interpretation of the references to color in this figure caption, the reader is referred to the web version of this paper.)

Please cite this article as: V. Pilipchuk, et al., Transient friction-induced vibrations in a 2-DOF model of brakes, *Journal of Sound and Vibration* (2015), http://dx.doi.org/10.1016/j.jsv.2015.01.028

with a top view is consequently used to process a `signal`. The spectrogram representation is convenient in the present case of temporal scales, although other methods, such as wavelet or Hilbert transforms can be applied as well for the purpose of processing such types of signals. Also, spectral characterization seems to be most reasonable in case of mechanical systems, since it gives a direct answer regarding possible resonance conditions. Fig. 4a and b represents spectrograms of the block coordinate x_1 obtained from the test record and numerical solution of (5).

There are some quantitative differences in terms of amplitudes, as expected due to the discussion at end of Section 3. However, major spectral lines of the diagrams in Fig. 4 are in a reasonable match with their levels reflecting the two principal frequencies of the linearized conservative system (see the beginning of Section 3). The natural frequencies are found to be $\omega_1 = 9.87007$ Hz and $\omega_2 = 14.1971$ Hz. The second one appears to be in a match with the corresponding spectral line, while the first frequency is somewhat higher than the spectral line. The spectral line is at level about 8 Hz by the visual estimates, because the next grid line is 13 Hz. The above natural frequencies are estimated from the linearized autonomous conservative system, and as such they do not have to exactly coincide with the spectral lines obtained from the test and simulations with the entire model. The entire model is non-autonomous, non-conservative, and non-linear, and its dynamic response may have quite different frequency contents due to different factors, i.e. third term in Eq. (6) or by neglecting friction force when calculating natural frequencies.

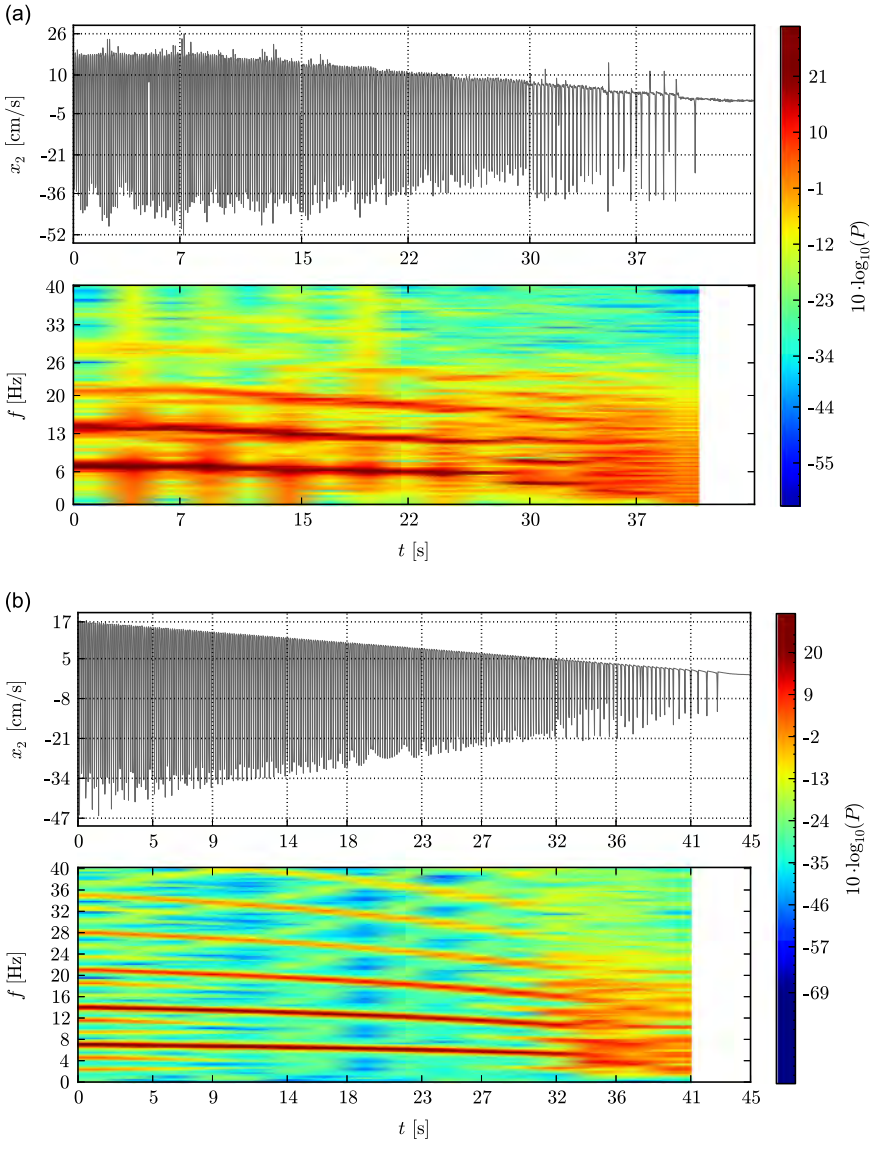

Fig. 5. Time histories of the main body velocity with the corresponding Matlab spectrograms obtained from (a) test and (b) numerical simulation for the theoretical model; see comments to Fig. 4 above.

Please cite this article as: V. Pilipchuk, et al., Transient friction-induced vibrations in a 2-DOF model of brakes, *Journal of Sound and Vibration* (2015), http://dx.doi.org/10.1016/j.jsv.2015.01.028

The bottom spectral line near zero corresponds to a constant component in the oscillating coordinate. Note a gradual decrease of the frequencies as the belt speed decelerating with time. Keeping in mind the discussion of Fig. 3, note also a significant spectral widening by the final phase of the process, which begins quite abruptly at about $t = 35$ s; see also Fig. 3b and d for a detailed characterization of temporal histories in this interval. In addition to the two major frequencies clearly seen in the interval $0 < t < 35$, there are several sub-harmonics however of much lower power; in spectrograms, a 'cooler' color represents lower amplitudes of the power spectral density. Similar illustrations are used for the block's speed in Fig. 5.

Sub-harmonics are seen more developed in this case since high frequency components produce a stronger contribution to the speed. The upper edge of the time history diagrams associated with the 'sticking' phase of vibrations actually reflects the belt speed; see Fig. 3a–d for details. It is seen that the real belt of the experimental rig does not perfectly follow that of the model, however, it is reasonably close to the target. Also, there are some irregular upward spikes in the test record for the block's velocity $x_2 = \dot{x}_1$; see also Fig. 3a and b. Such 'overshoots' mean that practically the block 'sticks' sometimes in a reverse mode. Such events are quite irregular and rather happen due to natural imperfections in the belt surface, fluctuations of the belt speed caused by its elasticity, as well as many other factors. Variations of the normal pressure on the block could also be a contributing factor; however, the model did not capture such effect, although it takes into account the normal pressure variations.

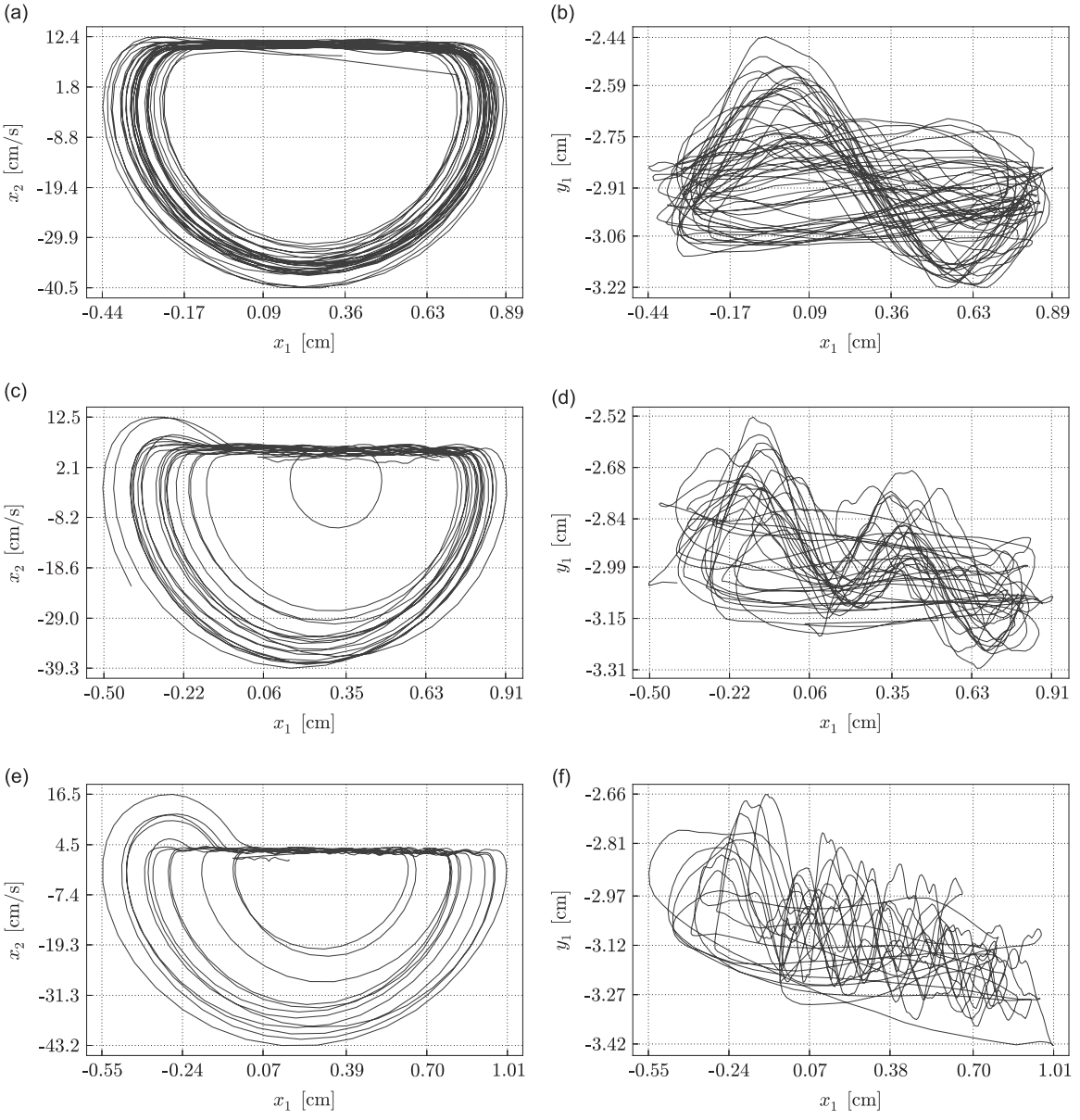

Fig. 6. Experimental records in different time windows for phase plane of (a, c, and e) the main block, and (b, d, and f) configuration plane of the model. (a) $20 < t < 25$, and (b) $20 < t < 25$, (c) $30 < t < 35$, (d) $30 < t < 35$, (e) $35 < t < 40$ and (f) $35 < t < 40$.

Please cite this article as: V. Pilipchuk, et al., Transient friction-induced vibrations in a 2-DOF model of brakes, *Journal of Sound and Vibration* (2015), http://dx.doi.org/10.1016/j.jsv.2015.01.028

Fig. 6a, c, e and b, d, f shows trajectories on the phase plane of main block and configuration plane of the system, respectively, in three different time windows of the same length 5 s obtained from the test. Typical stick-slip vibrations can be identified from the phase plain diagrams in Fig. 6a, c, and e. The horizontal part of every loop corresponds to the 'sticking' phase and therefore its level indicates the belt speed, which is gradually decreasing with time. This is also the reason why the loops have different sizes so that the diagrams look like a bunch of curves rather than an attractor. Similar effect is seen in configuration planes shown in Fig. 6b, d, and f, although configuration trajectories look more irregular due to contribution of the angular body. Nevertheless, 'fingerprints' of some attractors, corresponding to different frequency ratios, can be seen in fragments b and d of Fig. 6. Further, the irregularity is increasing by the end of the process as predicted already by the Fourier spectrograms and time histories. The elevation of some loops on the right of the phase plane diagrams correspond to the spikes as described in the discussion of Fig. 3.

Similar illustrations are shown in Fig. 7 based on numerical solutions. Although shapes of the curve and locations of time windows are somewhat different, qualitatively the evolution of trajectories is similar to that obtained from the test.

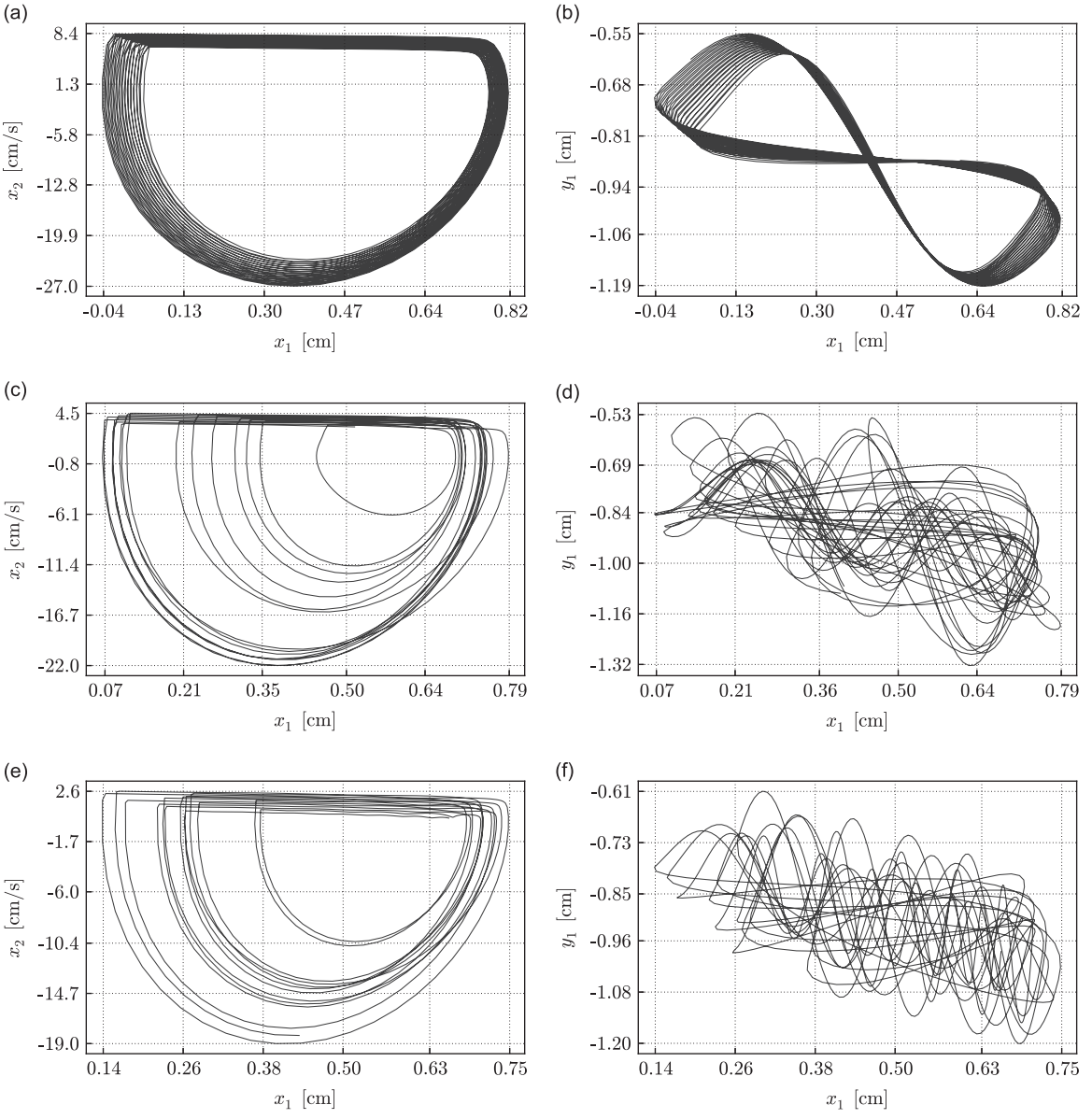

Fig. 7. Numerical solutions for the model shown in different time windows for phase plane of (a, c, and e) the main block and (b, d, and f) configuration plane of the model. (a) $23 < t < 28$, and (b) $23 < t < 28$, (c) $34 < t < 39$, (d) $34 < t < 39$, (e) $38 < t < 43$ and (f) $38 < t < 43$.

Please cite this article as: V. Pilipchuk, et al., Transient friction-induced vibrations in a 2-DOF model of brakes, *Journal of Sound and Vibration* (2015), http://dx.doi.org/10.1016/j.jsv.2015.01.028

5. Periodic attractors and modal transitions

The capability of the current test rig including multiple auxiliary mechatronic components does not allow sometimes to implement any conditions achievable in numerical tests. However, interesting effects revealed from numerical simulations can serve as a guideline for redesigning the rig and planning further experiments. From that standpoint, let us consider the model (5) under the assumption (11) regarding the belt speed with $V_0 = 0.25$ m s^{-1} and $T_{\max} = 160$ s. Although the initial speed is higher than that assumed in Section 4, the decay rate is lower due to the much longer deceleration interval. Such conditions are expected to allow different quasi attractors to develop more clearly and make observable transitional effects during the deceleration.

For instance, Fig. 8a–c illustrates the dynamics of angular body during the entire process that points to at least six different segments; compare the intervals $0 < t < 98$, $98 < t < 110$, $110 < t < 130$, $130 < t < 135$, $135 < t < 140$, and $140 < t < 150$, where the numbers are given in seconds, and the boundaries are indicated conditionally based on visual estimates. As follows from Fig. 9, the friction force F behaves in different ways within different segments, and this may affect the dynamics of entire system. In particular, Fig. 9a and b shows some decay of the amplitude of spike with a minor increase of the interval between them, as compared the initial and final phases of the first segment. However, the spike shapes remain qualitatively the same during the entire segment. Such a quasi steady-state dynamics during the first about 98 s is confirmed also by the Fourier spectrograms of the system coordinates in Fig. 10. The next relatively short interval, $98 < t < 110$, is characterized by quite irregular spiking behavior of the friction force as confirmed by the fragment in Fig. 9c.

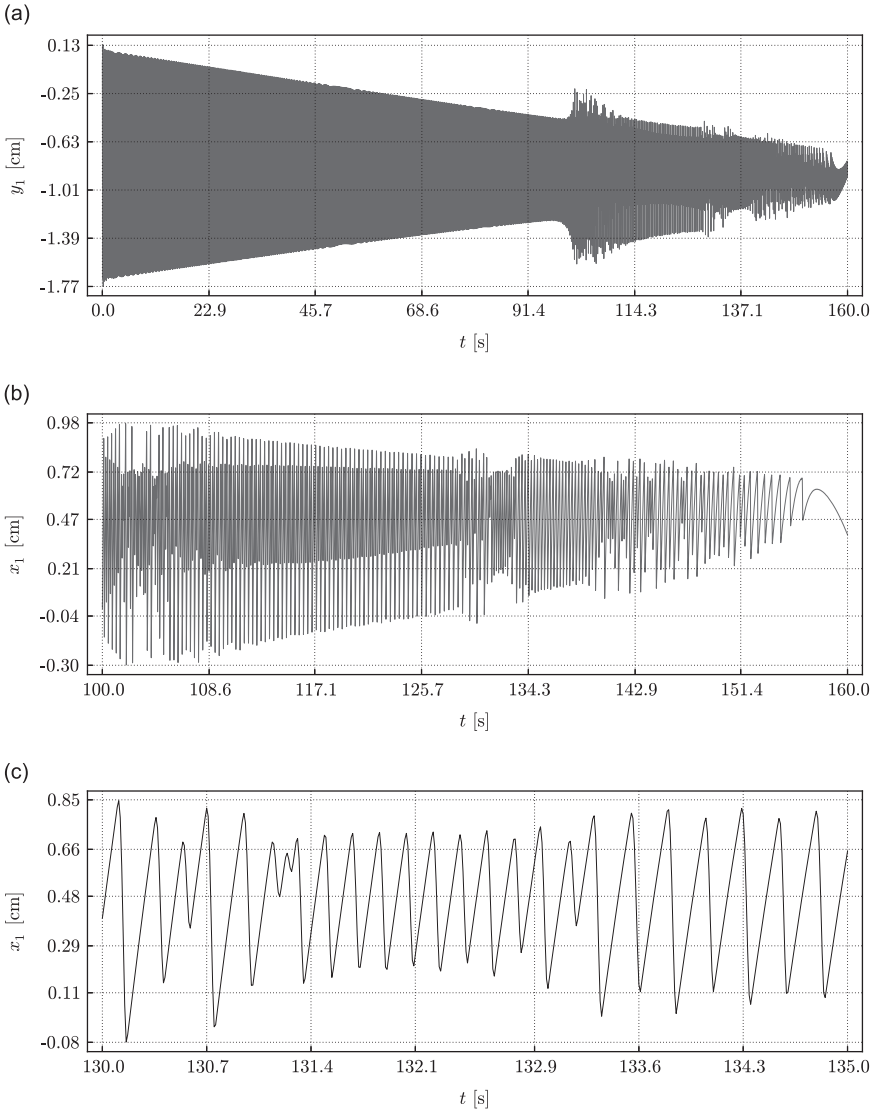

Fig. 8. Time history of the angular body position under the belt speed $V_0 = 0.25(1 - t/160)$m s^{-1}; different time windows (a–c) clearly show a sequence of different segments in the dynamics with transitional effects. (a) $0 < t < 160$, and (b) $100 < t < 160$ and (c) $130 < t < 135$.

Please cite this article as: V. Pilipchuk, et al., Transient friction-induced vibrations in a 2-DOF model of brakes, *Journal of Sound and Vibration* (2015), http://dx.doi.org/10.1016/j.jsv.2015.01.028

The Fourier spectrogram shows the corresponding narrow strip of widening spectrum; see Fig. 10a and b. The irregularity of motion is confirmed also by the diagrams in Fig. 11e and f. As follows from Figs. 9b, 11c and d, the onset of chaotic domain is accompanied by period doubling. The chaotic area ends at about $t=110$ by giving rise to a regular multiple frequency domain of about 20 s. Then another narrow strip of widening spectrum is observed before the next interval of regular multiple frequency motion. Interestingly enough, the frequency force spike shapes become similar to those within the first regular interval with somewhat lower frequencies though; compare Fig. 9e and b. Nevertheless, the motion modal contents are different; compare Fig. 11b and j. Finally, a wide strip of the dense spectrum begins at about $t=140$. Note that, in this case, the densifying spectrum is caused by the temporal localization of the friction force spikes rather than their irregularity; see Figs. 9f and 11k. Such rare force spikes support observable high frequency vibrations of the angle body between the spikes; see the configuration plane diagram in Fig. 11l. Such oscillations also lead to oscillations of the friction force due to the variations of normal load on the horizontal block; see Fig. 9f. It is remarkable that such higher frequency oscillations start forming, when the belt motion becomes very slow. Finally, comparing spectral lines of the spectrograms during different segments in Fig. 10 with diagrams in Fig. 11a and b, g and h, and i and j points to a series of modal transitions associated with different types of quasi attractors separated by narrow intervals of irregular motions. Further, Eq. (11) can help to identify the belt speed at which an attractor could practically develop at steady states under the constant belt speed.

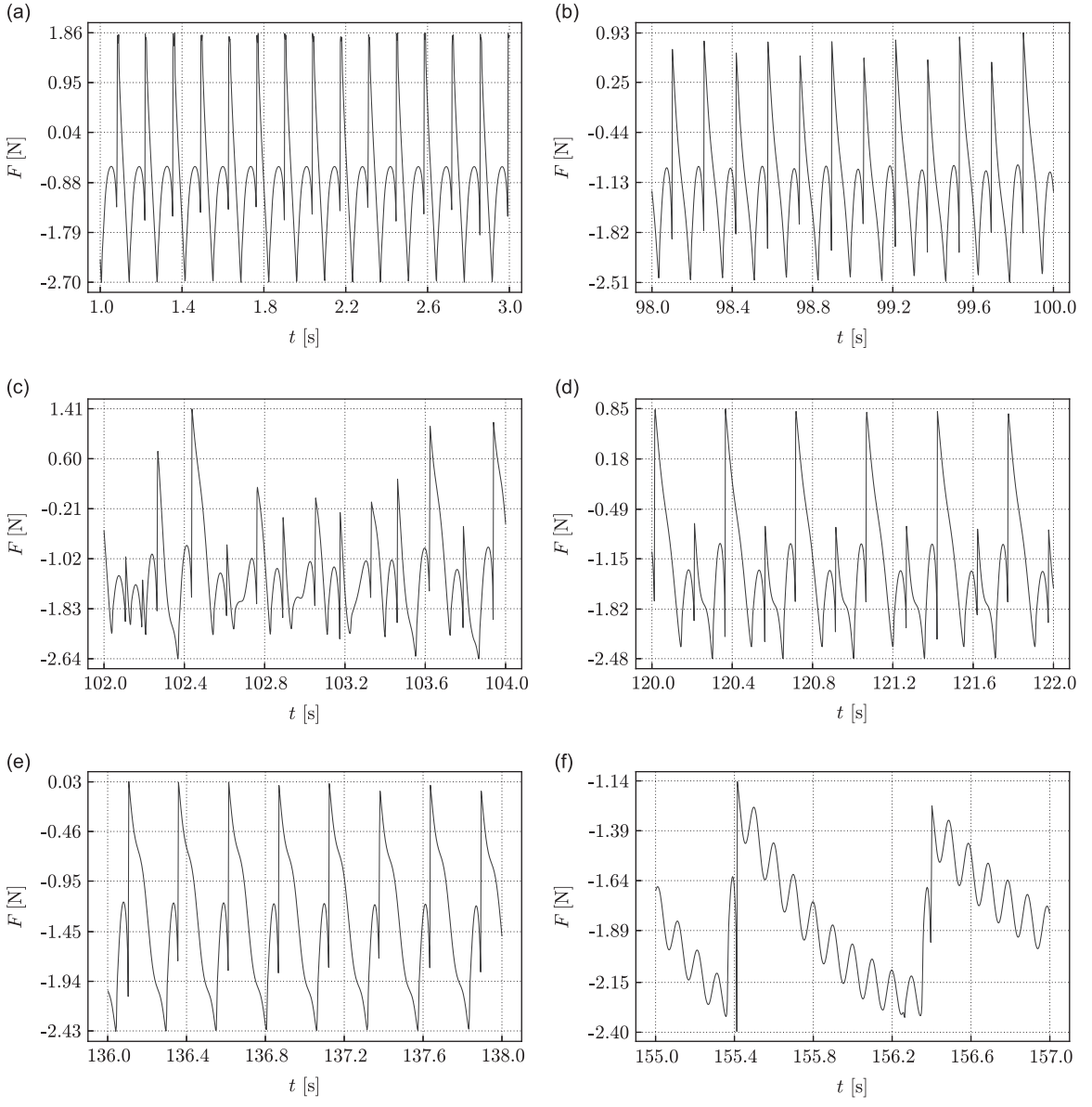

Fig. 9. Short-term temporal behaviors of friction force from different segments of the dynamics depicted in Fig. 8. (a) $1<t<3$, (b) $98<t<100$, (c) $102<t<104$, (d) $120<t<122$, (e) $136<t<138$, (f) $155<t<157$.

Please cite this article as: V. Pilipchuk, et al., Transient friction-induced vibrations in a 2-DOF model of brakes, *Journal of Sound and Vibration* (2015), http://dx.doi.org/10.1016/j.jsv.2015.01.028

6. Conclusions

In this work, based on the mechanical mass–spring–belt system and an experimental rig designed in [21], we obtained an experimental proof of transient effects in friction-induced vibrations revealed earlier theoretically in [25]. The mathematical model used in [21] is generalized here in order to account for geometrical nonlinearities and the influence of gravitation. This allowed us to obtain a reasonable qualitative match between theoretical and experimental results in terms of time histories of the dynamic states and transient spectral properties of vibrations. In particular, both experiment solution and numerical solution confirm the effect of densifying spectral bend by the final phase of deceleration process. In real brake systems with much high and denser eigen-frequencies, the densifying spectral bend becomes more likely to cover some of the acoustic modes with generation of squeal. Numerical simulations with a very gradual belt deceleration reveal the hierarchy of modal transitions associated with different quasi steady-state multiple frequency vibrations separated by relatively narrow time intervals of irregular dynamics.

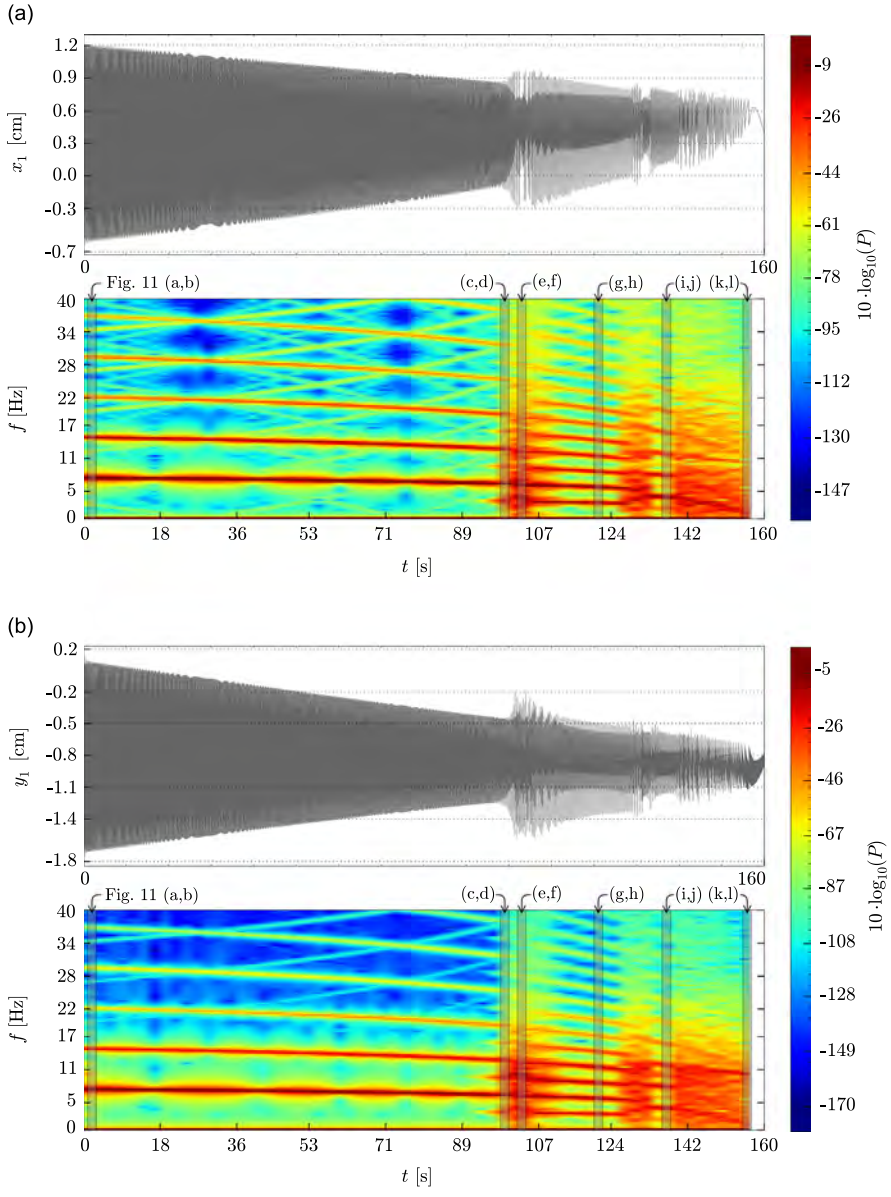

Fig. 10. Time history with the corresponding Fourier spectrograms under the belt speed (11) for $V_0 = 0.25\ \mathrm{m\ s^{-1}}$ and $T_{\max} = 160\ \mathrm{s}$: (a) main block and (b) angular body.

Please cite this article as: V. Pilipchuk, et al., Transient friction-induced vibrations in a 2-DOF model of brakes, *Journal of Sound and Vibration* (2015), http://dx.doi.org/10.1016/j.jsv.2015.01.028

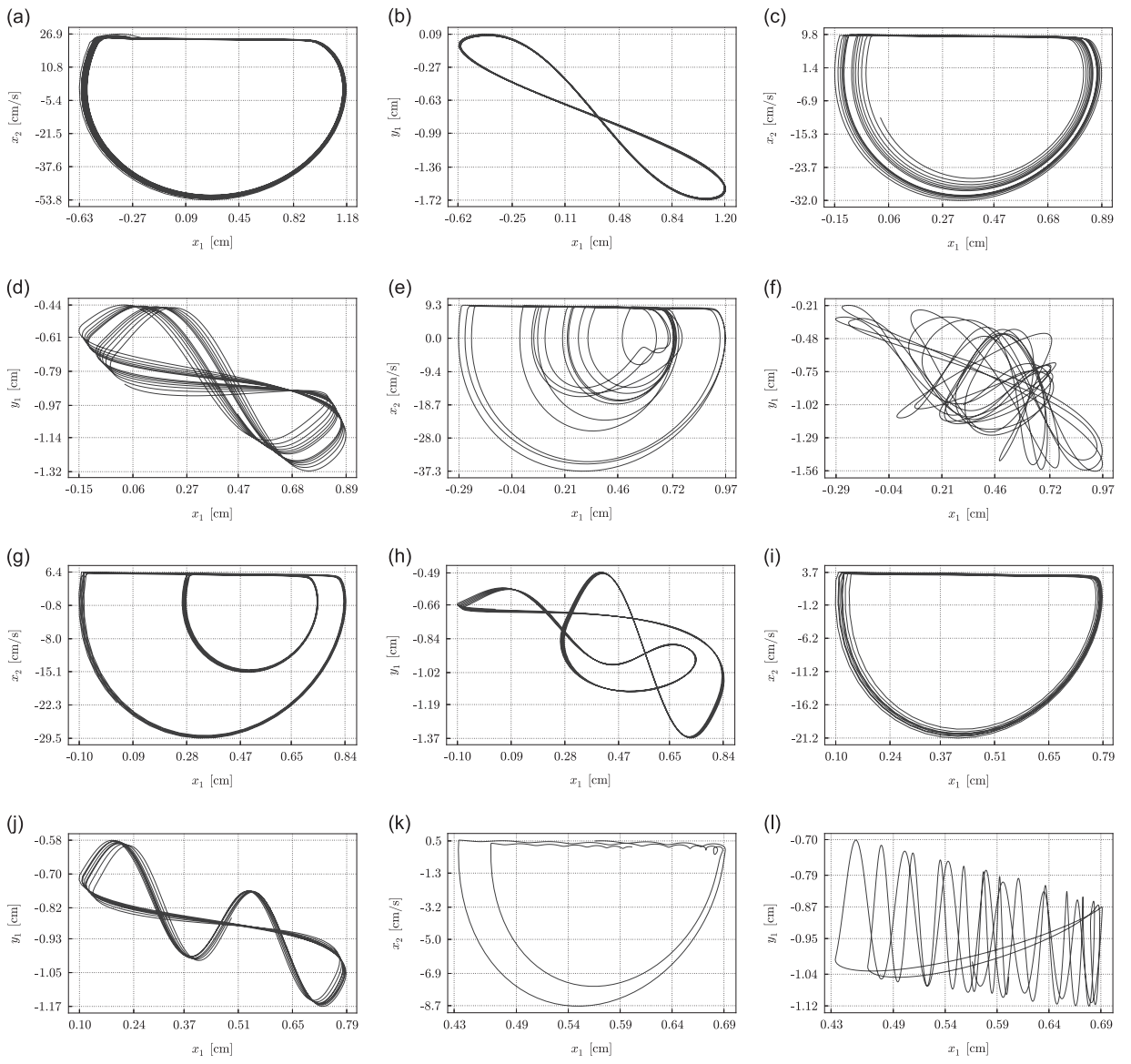

Fig. 11. Numerical solutions for the model shown in different time windows at the belt speed (11) for $V_0 = 0.25$ m s^{-1} and $T_{\max} = 160$ s: (a, c, e, g, i, and k) phase plane of the main block and (b, d, f, h, j, and l) configuration plane of the model. (a) $1 < t < 3$, and (b) $1 < t < 3$, (c) $98 < t < 100$, (d) $98 < t < 100$, (e) $102 < t < 104$, (f) $102 < t < 104$, (g) $120 < t < 122$, (h) $120 < t < 122$, (i) $136 < t < 138$, (j) $136 < t < 138$, (k) $155 < t < 157$ and (l) $155 < t < 157$.

Acknowledgments

The authors P. Olejnik and J. Awrejcewicz have been supported by the National Center of Science under the Grant MAESTRO 2, No. 2012/04/A/ ST8/00738 for years 2012–2015 (Poland).

References

[1] G.G. Adams, Self-excited oscillations in sliding with a constant friction coefficient—a simple model, *ASME Journal of Tribology* 118 (1996) 819–823.
[2] G.G. Adams, Radiation of body waves induced by the sliding of an elastic half-space against a rigid surface, *ASME Journal of Applied Mechanics* 67 (2000) 1–5.
[3] G.G. Adams, M. Nosovsky, Contact modeling—forces, *Tribology International* 33 (2000) 431–442.
[4] A. Akay, Acoustics of friction, *Journal of the Acoustical Society of America* 111 (2002) 1525–1548.
[5] J. Awrejcewicz, I. Andrianov, L. Manevitch, *Asymtotic Approach in Nonlinear Dynamics: New Trends and Applications*, Springer, Berlin, 1998.
[6] J. Awrejcewicz, J. Delfs, Dynamics of a self-excited stick-slip oscillator with two degrees of freedom. Part I: *investigation of equilibria*, *European Journal of Mechanics, A/Solids* 9 (1990) 269–282.

Please cite this article as: V. Pilipchuk, et al., Transient friction-induced vibrations in a 2-DOF model of brakes, *Journal of Sound and Vibration* (2015), http://dx.doi.org/10.1016/j.jsv.2015.01.028

[7] J. Awrejcewicz, J. Delfs, Dynamics of a self-excited stick-slip oscillator with two degrees of freedom. Part II: *slip-stick, slip-slip, stick-slip transitions, periodic and chaotic orbits*, *European Journal of Mechanics, A/Solids* 9 (1990) 397–418.
[8] J. Awrejcewicz, P. Olejnik, Analysis of dynamic systems with various friction laws, *Applied Mechanics Reviews—Transactions of ASME* 58 (2005) 389–411.
[9] J. Awrejcewicz, P. Olejnik, Friction pair modeling by 2-DOF system: *numerical and experimental investigations*, *International Journal of Bifurcations and Chaos* 15 (2005) 1931–1944.
[10] M.T. Bengisu, A. Akay, Stability of friction-induced vibrations in multi-degree-of-freedom systems, *Journal of Sound and Vibration* 171 (1994) 557–570.
[11] J.R. Bristow, Kinetic boundary friction, *Proceedings of Royal Society of London, Series A* 189 (1947) 88–102.
[12] J.P. Den Hartog, *Mechanical Vibrations*, McGraw-Hill, New York, 1956.
[13] B. Feeny, F.C. Moon, Chaos in a forced dry friction oscillator: *experiment and numerical modelling*, *Journal of Sound and Vibration* 170 (1994) 303–323.
[14] A.F. Filippov, *Differential Equations with Discontinuous Right-Hand Side, Mathematics and Its Applications*, Kluwer Academic Publishers, Dordrecht, 1988.
[15] U. Galvanetto, S.R. Bishop, Stick-slip vibrations of a two-degrees-of-freedom geophysical fault model, *International Journal of Mechanical Sciences* 36 (1994) 683–698.
[16] R.A. Ibrahim, Friction-induced vibration, chatter, squeal, and chaos. Part I: *mechanics of contact and friction*, *ASME Applied Mechanics Reviews* 47 (1994) 209–226.
[17] R.A. Ibrahim, Friction-induced vibration, chatter, squeal, and chaos. Part II: *dynamics and modeling*, *ASME Applied Mechanics Reviews* 47 (1994) 227–253.
[18] N.M. Kinkaid, O.M. O'Reilly, P. Papadopoulos, On the transient dynamics of a multi-degree-of-freedom friction oscillator: *a new mechanism for disc brake noise*, *Journal of Sound and Vibration* 287 (2005) 901–917.
[19] L. Knopoff, J.A. Landoni, M.S. Abinante, Dynamical model of an earthquake fault with localization, *Physical Review A* 46 (1992) 7445–7449.
[20] M. Leamy, J.R. Barber, N.C. Perkins, Distortion of a harmonic elastic wave reflected from a dry friction support, *ASME Journal of Applied Mechanics* 65 (1998) 851–857.
[21] P. Olejnik, Numerical and Experimental Analysis of Self-Excited Regular and Chaotic Vibrations in a Two Degrees of Freedom System, PhD Thesis, Lodz University of Technology, Lodz, 2002 (in Polish).
[22] P. Olejnik, J. Awrejcewicz, Application of Hénon method in numerical estimation of the stick-slip transitions existing in Filippov-type discontinuous dynamical systems with dry friction, *Nonlinear Dynamics* 73 (2013) 723–736.
[23] G. Ostermeyer, Dynamic Friction Laws and their Impact on Friction Induced Vibrations, Technical Report 2010-01-1717, SAE Technical Paper, http://dx.doi.org/10.4271/2010-01-1717, 2010.
[24] V.N. Pilipchuk, R.A. Ibrahim, P.G. Blaschke, Disc brake ring-element modeling involving friction-induced vibration, *Journal of Vibration and Control* 8 (2002) 1085–1104.
[25] V.N. Pilipchuk, C.A. Tan, Stick-slip capture and source of squeal at decelerating sliding, *Nonlinear Dynamics* 35 (2004) 259–285.
[26] K. Popp, P. Stelter, Stick-slip vibrations and chaos, *Philosophical Transactions of the Royal Society A. Philosophical Transactions A* 332 (1990) 89–105.
[27] V.B. Ryabov, H.M. Ito, Multistability and chaos in a spring–block model, *Physical Review E* 52 (1995) 6101–6112.
[28] S.W. Shaw, On the dynamic response of a system with dry friction, *Journal of Sound and Vibration* 108 (1986) 305–325.
[29] J.-J. Sinou, O. Dereure, G.-B. Mazet, F. Thouverez, L. Jezequel, Friction-induced vibration for an aircraft brake system—Part 1: experimental approach and stability analysis, *International Journal of Mechanical Sciences* 48 (2006) 536–554.
[30] D.M. Tolstoi, Significance of the normal degree of freedom and natural normal vibrations in contact friction, *Wear* 10 (1967) 199–213.
[31] O. Vahid-Araghi, F. Golnaraghi, *Friction-Induced Vibration in Lead Screw Drives*, Springer, New York, 2011.
[32] P. Vielsack, Stick-slip instability of decelerative sliding, *International Journal of Non-Linear Mechanics* 36 (2001) 237–247.
[33] B. Wikiel, J.M. Hill, Stick-slip motion for two coupled masses with side friction, *International Journal of Non-Linear Mechanics* 35 (2000) 953–962.

Please cite this article as: V. Pilipchuk, et al., Transient friction-induced vibrations in a 2-DOF model of brakes, *Journal of Sound and Vibration* (2015), http://dx.doi.org/10.1016/j.jsv.2015.01.028